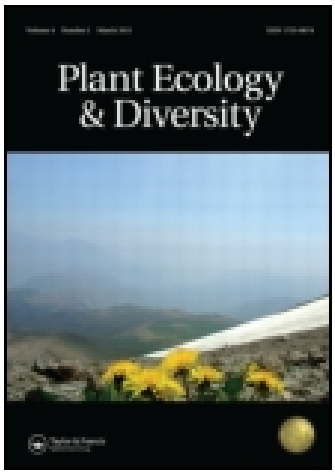

Plant Ecology & Diversity
Publication details, including instructions for authors and subscription information:
http://www.tandfonline.com/loi/tped20

Seasonal production, allocation and cycling of carbon in two mid-elevation tropical montane forest plots in the Peruvian Andes

Walter Huaraca Huasco [a], Cécile A.J. Girardin [b], Christopher E. Doughty [b], Daniel B. Metcalfe [c], Liliana D. Baca [a], Javier E. Silva-Espejo [a], Darcy G. Cabrera [a], Luiz E.O.C. Aragão [d], Angela R. Davila [a], Toby R. Marthews [b], Lidia P. Huaraca-Quispe [a], Ivonne Alzamora-Taype [a], Luzmila E. Mora [a], William Farfán-Rios [e], Karina G. Cabrera [e], Katherine Halladay [b], Norma Salinas-Revilla [a b], Miles R. Silman [e], Patrick Meir [f] & Yadvinder Malhi [b]

[a] Universidad Nacional de San Antonio Abad del Cusco , Cusco , Peru

[b] Environmental Change Institute , University of Oxford , Oxford , UK

[c] Department of Forest Ecology and Management , Swedish University of Agricultural Sciences , Umeå , Sweden

[d] College of Life and Environmental Sciences , University of Exeter , Exeter , UK

[e] Center for Energy, Environment, and Sustainability , Wake Forest University , North Carolina , USA

[f] School of Geosciences , University of Edinburgh , Edinburgh , UK

Published online: 16 Sep 2013.

To cite this article: Walter Huaraca Huasco , Cécile A.J. Girardin , Christopher E. Doughty , Daniel B. Metcalfe , Liliana D. Baca , Javier E. Silva-Espejo , Darcy G. Cabrera , Luiz E.O.C. Aragão , Angela R. Davila , Toby R. Marthews , Lidia P. Huaraca-Quispe , Ivonne Alzamora-Taype , Luzmila E. Mora , William Farfán-Rios , Karina G. Cabrera , Katherine Halladay , Norma Salinas-Revilla , Miles R. Silman , Patrick Meir & Yadvinder Malhi (2014) Seasonal production, allocation and cycling of carbon in two mid-elevation tropical montane forest plots in the Peruvian Andes, Plant Ecology & Diversity, 7:1-2, 125-142, DOI: 10.1080/17550874.2013.819042

To link to this article: http://dx.doi.org/10.1080/17550874.2013.819042

Plant Ecology & Diversity, 2014
Vol. 7, Issues 1–2, 125–142, http://dx.doi.org/10.1080/17550874.2013.819042

Taylor & Francis
Taylor & Francis Group

Seasonal production, allocation and cycling of carbon in two mid-elevation tropical montane forest plots in the Peruvian Andes

Walter Huaraca Huasco[a], Cécile A.J. Girardin[b]*, Christopher E. Doughty[b], Daniel B. Metcalfe[c], Liliana D. Baca[a], Javier E. Silva-Espejo[a], Darcy G. Cabrera[a], Luiz E.O.C. Aragão[d], Angela R. Davila[a], Toby R. Marthews[b], Lidia P. Huaraca-Quispe[a], Ivonne Alzamora-Taype[a], Luzmila E. Mora[a], William Farfán-Rios[e], Karina G. Cabrera[e], Katherine Halladay[b], Norma Salinas-Revilla[a,b], Miles R. Silman[e], Patrick Meir[f] and Yadvinder Malhi[b]*

[a]*Universidad Nacional de San Antonio Abad del Cusco, Cusco, Peru;* [b]*Environmental Change Institute, University of Oxford, Oxford, UK;* [c]*Department of Forest Ecology and Management, Swedish University of Agricultural Sciences, Umeå, Sweden;* [d]*College of Life and Environmental Sciences, University of Exeter, Exeter, UK;* [e]*Center for Energy, Environment, and Sustainability, Wake Forest University, North Carolina, USA;* [f]*School of Geosciences, University of Edinburgh, Edinburgh, UK*

(*Received 20 March 2012; final version received 19 June 2013*)

Background: Tropical montane cloud forests (TMCF) are unique ecosystems with high biodiversity and large carbon reservoirs. To date there have been limited descriptions of the carbon cycle of TMCF.
Aims: We present results on the production, allocation and cycling of carbon for two mid-elevation (1500–1750 m) tropical montane cloud forest plots in San Pedro, Kosñipata Valley, Peru.
Methods: We repeatedly recorded the components of net primary productivity (*NPP*) using biometric measurements, and autotrophic (R_a) and heterotrophic (R_h) respiration, using gas exchange measurements. From these we estimated gross primary productivity (*GPP*) and carbon use efficiency (*CUE*) at the plot level.
Results: The plot at 1500 m was found very productive, with our results comparable with the most productive lowland Amazonian forests. The plot at 1750 m had significantly lower productivity, possibly because of greater cloud immersion. Both plots had similar patterns of *NPP* allocation, a substantial seasonality in *NPP* components and little seasonality in R_a.
Conclusions: These two plots lie within the ecotone between lower and upper montane forests, near the level of the cloud base. Climate change is likely to increase elevation of the cloud base, resulting in shifts in forest functioning. Longer-term surveillance of the carbon cycle at these sites would yield valuable insights into the response of TMCFs to a shifting cloud base.

Keywords: Andes; ecophysiology; elevational gradient; gross primary productivity; net primary productivity; carbon use efficiency; soil water content; temperature; tropical montane forests

Introduction

The fixation of carbon through gross primary productivity (*GPP*) and its respiration through autotrophic and heterotrophic processes in tropical forests are important aspects of the global carbon cycle. These variables have been investigated in lowland tropical forests, but they have rarely been studied in tropical montane forests. Tropical montane forests typically maintain lower above-ground productivity, lower soil nutrient concentrations and slower nutrient turnover than tropical lowland forests (Bruijnzeel and Proctor 1995; Benner et al. 2010).

To date, most studies of tropical forest carbon cycling have focused on above-ground components of net primary productivity (*NPP*), such as wood productivity (e.g. Malhi et al. 2004) and litterfall (e.g. Chave et al. 2009). Recently, a more comprehensive approach to intensive carbon cycling surveillance has been the focus of a network of plots in lowland Amazonia. This approach provides a comprehensive assessment of ecosystem carbon dynamics over an annual cycle, from the rate of fixation of CO_2 by photosynthesis in the canopy (*GPP*) to the rate of assimilation into biomass (*NPP*) and emission through autotrophic and heterotrophic respiration (R_a and R_h). Measuring each component of the carbon cycle independently allows us to improve the mechanistic understanding of how these components interact internally and with environmental parameters, and to cross-check with other component measurements for internal consistency in the carbon budget.

Tropical montane forests may be highly sensitive to climate change as temperatures and cloud bases rise, so understanding how processes vary along a tropical elevation gradient can provide fundamental new insights into how temperature controls ecosystem processes and function (Malhi et al. 2010). Here, we present the first comprehensive data set of carbon cycling for a tropical montane forest. We present results from two 1 ha permanent plots in south-eastern Peru, at elevations of 1500 m and 1750 m a.s.l., a zone that is close to mean cloud base altitude in the austral winter and the boundary between the lower montane and upper montane (cloud forest) forest zones, defined by the transition from partial to frequent cloud cover along the eastern escarpment of the Andes. We compared seasonal

*Corresponding authors. Email: cecile.girardin@ouce.ox.ac.uk; yadvinder.malhi@ouce.ox.ac.uk

cycles of production, allocation and cycling of carbon at two mid-elevational tropical forest plots in the Peruvian Andes. We asked the following research questions:

(1) How do the components of *NPP* and R_a of these forests vary over the seasonal cycle and what are their main climatic drivers?
(2) What are the seasonal trends of total plant carbon expenditure and carbon use efficiency (*CUE*) at both plots?
(3) How do the annual carbon budgets (defined as *NPP*, R_a, *GPP* and *CUE*) compare between these two plots in close proximity, both located at the base of the cloud cover?

Materials and methods

Site characteristics

The San Pedro site (13° 2′ 53″ S, 71° 32′ 23″ W) is located in the Kosñipata Valley, in the cultural buffer zone of the Parque Nacional del Manú, Cusco, Peru (Table 1). Since 2003, the Andes Biodiversity Ecosystems Research Group (ABERG, andesresearch.org) has operated a number of permanent 1-ha plots in the Kosñipata Valley (Malhi et al. 2010): eight along the Trocha Union ridge-top trail (1855–3500 m a.s.l.), two at the Estación Biológica de Wayqecha (2825–3025 m a.s.l.) and two at San Pedro (1500 and 1750 m a.s.l.) where the valley enters the Madre de Dios region of Peru. Partial results from the San Pedro plot at 1500 m a.s.l. have been reported in previous papers: soil carbon stocks in Zimmermann et al. (2009, 2010), forest above-ground productivity in Girardin et al. (2010), modelling studies in Marthews et al. (2012), leaf decomposition in Salinas et al. (2011), stem respiration in Robertson et al. (2010) and the seasonality of below-ground productivity in Girardin et al. (unpublished). Here we provide the first comprehensive description (and an extended time series) of the carbon cycling at San Pedro at 1500 m (SP 1500), and the first data from 1750 m (SP 1750).

With low wood density (0.55 ± 0.01/0.61 ± 0.008 g cm^{-3} ha^{-1}), a predominance of taxa from lowland rainforests (e.g. Anacardiaceae, Moraceae, Myristicaceae), the abundance of fast-growing species (e.g. *Tachigali* spp., *Tapirira* spp., *Alchornea* spp.), little occurrence of classic dominant cloud forest species (e.g. *Weinmannia* spp.), little occurrence of tree ferns and epiphytes, the plant composition of SP 1500 is closer to that of sub-montane to lowland tropical forests (Rapp and Silman 2012). SP 1750 has ecological species composition typical of montane cloud forests, with a high tree fern incidence (a good indicator of cloud immersion zone), a high occurrence of *Weinmannia* spp. (e.g. *W. lechleriana*, *W. pinnata*), and the prevalence of stem-covering bryophytes (A. Horwath, pers comm. 2012).

The climate of both plots is characterised by very high rainfall (5300 mm $year^{-1}$), no distinct dry season, and periods of cloud immersion. Cloud base is lowest in the austral winter/dry season (May–July) and rises in the austral summer/wet season (K. Halladay 2012, pers comm.). Relative humidity (RH) is highest in austral winter, owing to an increased frequency of cloud immersion because of lower cloud base altitude; this reduces to a minimum in September as cloud base height increases and before the onset of the wet season. On a diurnal basis, cloud base altitude decreases from morning to afternoon as a result of moist upslope flow from the lowlands (K. Halladay 2012, pers comm.). Hence in the austral winter these plots are occasionally immersed in cloud, with a larger degree of immersion in the higher elevation plot. This proximity to the cloud base zone (which may be expected to rise under

Table 1. Characteristics of the San Pedro permanent forest plots in the Kosñipata National Park, Cusco, Peru. Organic layer depth derived from Zimmermann et al. (2009); soil carbon stock from A. Quesada (pers. comm.); weather data derived from SOTERLAC (Dijkshoorn et al. 2005) and K. Halladay (pers. comm.).

Site Name	San Pedro 1500 m a.s.l.	San Pedro 1750 m a.s.l.
RAINFOR Site Code	SPD-02	SPD-01
Latitude	−13.049	−13.047
Longitude	−71.537	−71.542
Elevation (meters above sea level)	1500	1750
Mean annual air temperature (°C)	18.80 ± 0.02	17.43 ± 0.02
Annual precipitation (mm $year^{-1}$)	5302	5302
Solar radiation (GJ m^{-2} $year^{-1}$)	4.08	4.36
Mean climatological water deficit (mm mo^{-1})	−15.0	−15.0
Aspect	West-facing	West-facing
Soil organic layer depth (L, H, O, cm)	10.48 ± 1.11	12.44 ± 1.40
Geology	Late Permian granite intrusions	Late Permian granite intrusions
Soil order	Umbrisol	Umbrisol
pH (in water, 1:2.5)	4.0	–
Readily available P (mg/kg)	8648	–
Soil C (%)	15.2	–
Canopy height (all trees <40 cm DBH, meters)	18	20
Dominant species	*Tachigali setifera, Tapirira* sp., *Alchornea latifolia*, *Miconia* sp.	*Tapirira guianensis, Alzatea verticilada, Helicostylis tovarensis*

global warming) makes these sites particularly interesting for ecological monitoring.

The soils in both plots are umbrisols, ca. 67 cm deep, with an organic layer of ca. 30 cm (Table 1). The soils are highly acidic (pH 4.0; Zimmerman et al. 2009), overlaying a late Permian granite intrusion bedrock. The vegetation is closed canopy forest with a relatively low mean canopy height (estimated as height of trees with diameter at breast height (DBH) > 40 cm, 18 ± 3 m for SP 1500, and 20 ± 3 m for SP 1750) and moderately high plant species diversity of trees >10 cm DBH (211 species in SP 1500, and 177 species in SP 1750). There were few differences between soil types, chemistry or physical characteristics between the two plots.

Meteorological data

Solar radiation, air temperature, humidity and precipitation time series were collected from an automatic weather station (AWS) installed in a clearing ca. 1 km from SP 1500. The monthly time series were then gap-filled. For solar radiation, the monthly mean value for each missing month was used to gap-fill. For temperature, daily values from a nearby Senamhi (Peruvian Meteorological Service) station at Acjanaco (13.20° S, 71.62° W) were regressed against daily values from the AWS to correct for the difference between these two stations. The monthly temperature time series was then gap-filled with corrected values from the Senamhi station. RH was calculated from wet and dry bulb temperatures, also from Acjanaco and measured at 07.00 h, 13.00 h and 19.00 h (local time) which were not adjusted. Any temperature or RH values that were still missing after gap-filling with Senamhi data were filled using monthly means from the partially filled time series. The precipitation time series was gap-filled by using values from the Senamhi station Acjanaco at 07.00 h and 19.00 h (local time) which were aggregated to produce monthly estimates. If fewer than the maximum possible number of daily values were available, the monthly value was considered to be missing. Where these data were missing, monthly values from the nearest grid point of the TRMM (Tropical Rainfall Measuring Mission) 3B43 product were used. Maximum climatic water deficit (MCWD), a measure of dry season intensity, was calculated, using the gap-filled monthly time series for precipitation according to the equations listed in Aragão et al. (2007).

Carbon fluxes

The protocols used to estimate ecosystem C flux components were largely based on those developed by the RAINFOR–GEM network. A detailed description is available online for download (http://gem.tropicalforests.ox.ac.uk) and in the online supplementary material accompanying this paper. Summaries of the different components quantified, and the field methods and data processing techniques used are presented in Tables 2 and 3, respectively.

Net primary productivity

All major *NPP* components were measured for this study in each of 25 subplots in each plot. We calculated above- and below-ground *NPP*, NPP_{AG} and NPP_{BG}, respectively, using the following equations:

$$NPP_{AG} = NPP_{ACW} + NPP_{litter\ fall} + NPP_{branch\ turnover} + NPP_{herbivory} \quad (1)$$

$$NPP_{BG} = NPP_{fine\ roots} + NPP_{coarse\ roots} \quad (2)$$

This neglects several small *NPP* terms, such *NPP* lost as volatile organic emissions, litter decomposed in the canopy, or dropped from ground flora below the litter traps. Total R_a is estimated as:

$$R_a = R_{leaves} + R_{stems} + R_{rhizosphere} \quad (3)$$

Here we count root exudates and transfer to mycorrhizae as a portion of $R_{rhizosphere}$ rather than as *NPP*. In quasi-steady state conditions (and on annual timescales or longer where there is no net change in plant non-structural carbohydrate storage), *GPP* should be approximately equal to plant carbon expenditure (*PCE*). Hence, we estimated *GPP* on the control plot as:

$$GPP = NPP_{AG} + NPP_{BG} + R_a \quad (4)$$

Using these data, we estimated the *CUE* as the proportion of total *GPP*/*PCE* invested in total *NPP*:

$$CUE = (NPP_{AG} + NPP_{BG})/(NPP_{AG} + NPP_{BG} + R_a) \quad (5)$$

Statistical analysis and error estimation

Repeated-measures analysis of variance (ANOVA) was used to test for significant seasonal shifts in ecosystem carbon components between plots. In addition, a student's *t*-test assessed mean annual differences between the two plots. Repeated-measures ANOVA was used to test both for significant seasonal shifts in ecosystem C components and for multiannual shifts in NPP_{ACW} measured every few months since 2009, between plots. In addition, a student's *t*-test assessed mean annual differences between the two plots.

All estimated fluxes reported in this study are in Mg C ha^{-1} $year^{-1}$, and all reported errors show ± 1 SE. Errors were propagated by taking the square root of the sum of squared absolute errors for addition and subtraction, and relative errors for division and multiplication (Taylor et al. 1997; Malhi et al. 2009; Hughes and Hase 2010). This assumes that uncertainties are independent and normally distributed.

A key consideration is assignment and propagation of uncertainty in our up-scaling of measurements. There are

Table 2. Methods for intensive monitoring of carbon dynamics from the SP 1500 and SP 1750 permanent forest plots in the Kosñipata National Park, Cusco, Peru (see also online supplemental material and RAINFOR-GEM manual 2012).

	Component	Description	Sampling period	Sampling interval
Above-ground net primary productivity (NPP_{AG})	Above-ground coarse wood net primary productivity (NPP_{ACW})	Annual forest inventory: All trees ≥ 10 cm dbh censused to determine growth rate of existing surviving trees and rate of recruitment of new trees. Stem biomass calculated using the Chave et al. (2005) allometric equation for tropical wet forests, employing diameter, height and wood density data. Four 15 m × 15 m and one 20 m × 20 m subplots established to census small trees (2.5–10 cm DBH)	2007–2011 (SP 1500) 2009–2011 (SP 1750)	Every year (trees ≥ 10 cm DBH) Every 6 months (trees 2.5–10 cm DBH)
		Seasonal growth: dendrometers installed on all trees (≥10 cm DBH) in each plot to determine the spatial-temporal and seasonal variation in growth.	As above	Every 3 months
	Branch turnover net primary productivity ($NPP_{branch\ turnover}$)	Branches > 2 cm diameter (excluding those fallen from dead trees) were surveyed within four 1 m × 100 m transects; small branches were cut to include only the transect-crossing component, removed and weighed. Larger branches had their dimensions taken (diameter at three points) and all were assigned a wood density value according to their decomposition class (Harmon et al. 1995).	2009–2011	Every 3 months
	Litterfall net primary productivity ($NPP_{litterfall}$)	Litterfall production of dead organic material < 2 cm diameter was estimated by collecting litterfall in 0.25 m2 (50 cm × 50 cm) litter traps placed at 1 m above the ground at the centre of each of the 25 subplots (4 × 4 m) in each plot.	2007–2009	Every 14 days
	Leaf area index (LAI)	Canopy images recorded with a digital camera and hemispherical lens near the centre of each of the 25 subplots, at a standard height of 1 m, and during overcast conditions. LAI estimated from these images using CAN-EYE free software (https://www4.paca.inra.fr/can-eye).	2009–2010	Every month
	Loss to leaf herbivory ($NPP_{herbivory}$)	Leaves collected in the 25 litterfall traps in each plot were photographed prior to being dried. Leaf area was determined with ImageJ image analysis software to calculate the area of each individual leaf including the damage incurred by herbivory.	2008	Every 2 months
Below-ground net primary productivity (NPP_{BG})	Coarse root net primary productivity ($NPP_{coarse\ roots}$)	Not measured directly; estimated as 0.21 ± 0.03 of above-ground woody productivity, based on Jackson et al. (1996); Cairns et al. (1997).	n/a	Not directly measured
	Fine root net primary productivity ($NPP_{fine\ roots}$)	Sixteen ingrowth cores (mesh cages 12 cm diameter, to 30 cm depth) were installed in each plot. Cores were extracted and roots were manually removed from the soil samples in four 10 min time steps and the pattern of cumulative extraction over time was used to predict root extraction beyond 40 min. Root-free soil was then re-inserted into the ingrowth core. Collected roots were thoroughly rinsed, oven dried at 80 °C to constant mass, and weighed. This process was repeated for each measurement thereafter.	2007–2011 (SP 1500) 2009–2011 (SP 1750)	Every 3 months

(*Continued*)

Table 2. (*Continued*)

	Component	Description	Sampling period	Sampling interval
Autotrophic and heterotrophic respiration (R_a and R_h)	Total soil CO_2 efflux (R_{soil})	Total soil CO_2 efflux was measured using a closed dynamic chamber method with an infra-red gas analyser and soil respiration chamber (EGM-4 IRGA and SRC-1 chamber, PP Systems, Hitchin, UK) sealed to a permanent collar in the soil. Soil surface temperature was measured with a T260 probe, Testo Ltd, Hampshire and soil moisture was recorded with a Hydrosense probe, Campbell Scientific Ltd.	2007–2011 (SP 1500) 2009–2011 (SP 1750)	Every month
	Soil CO_2 efflux partitioned into autotrophic ($R_{rhizosphere}$) and heterotrophic ($R_{soilhet}$) components	We installed soil respiration partitioning experiments at each corner of the plot. In each corner, we installed three short collar tubes (10 cm depth) to measure total soil respiration and three long collar tube (40 cm depth) to exclude root and mycorrhizae respiration (R_a) Each of the three tubes were allocated different litter layer treatments (normal litter, no litter, double litter). A control experiment was carried out at the centre of each plot in order to assess the effects of root severing and soil structure disturbance that occurs during installation.	Feb 2009–Jun 2011	Every month
	Canopy respiration (R_{leaves})	In each plot, leaf dark respiration and photosynthesis at PAR levels of 1000 μmol m^{-2} s^{-1} were recorded for 15–25 trees with an IRGA and specialised cuvette (CIRAS 2 IRGA with PLC6 leaf cuvette; PP Systems, Hitchen, UK). For each tree, we randomly selected one branch, each from sunlit and shaded portions of the canopy and immediately re-cut the branches underwater to restore hydraulic connectivity (Reich et al. 1998).	Nov 2010 and Jul 2011	Once in dry season, once in wet season
	Above-ground live wood respiration (R_{stems})	Bole respiration was measured using a closed dynamic chamber method, from 25 trees distributed evenly throughout each plot at 1.3 m height with an IRGA (EGM-4) and soil respiration chamber (SRC-1) connected to a permanent collar, sealed to the tree bole surface.	Mar 2009–Dec 2010	Every month
	Coarse root respiration ($R_{coarse\ roots}$)	This component of respiration was not measured directly.	n/a	Not directly measured

two primary types of uncertainty. First, there is the sampling error associated with spatial variation in the variables measured. Examples include the variability among litter traps, or among fine root ingrowth cores. Second, there is measurement uncertainty due to equipment functioning, measurement accuracy and, particularly, scaling localised measurement to tree and plot-level estimates. Here we assume that most *NPP* terms are measured fairly precisely and sampled without large biases, and hence *NPP* error is dominated by sampling uncertainty, which can be reliably estimated assuming a normal distribution. In contrast, we believe that the main R_a terms include a large measurement and scaling uncertainty, though these are very difficult to directly quantify. For these, we made explicit and conservative estimates of the combined measurement/scaling uncertainty for these components in Table 4. Some components were not directly measured at the site over the study period but were estimated from literature syntheses ($R_{coarse\ roots}$, $NPP_{coarse\ roots}$).

Results

We consistently report results from 1500 m first, followed by those from 1750 m, and for brevity we separate the two values by an oblique sign (/).

Abiotic environmental parameters

The average annual rainfall was very high (5302 mm), amongst the highest reported for any research site in

Table 3. Data analysis techniques for intensive monitoring of carbon dynamics from the SP 1500 and SP 1750 permanent montane forest plots in the Kosñipata national park, Cusco, Peru (see also online supplemental material and RAINFOR-GEM manual 2012).

	Component	Data processing details
Above-ground net primary productivity (NPP_{AG})	Above-ground coarse wood net primary productivity (NPP_{ACW})	Biomass calculated using the Chave et al. (2005) allometric equation for tropical moist forests: $\mathrm{AGB} = 0.0776 \times (\rho\ \mathrm{dbh}^2\ \mathrm{H})^{0.94}$, where AGB is above-ground biomass (kg), ρ is density of wood (g cm^{-3}), D is DBH (cm), and H is height (m). To convert biomass values into carbon, we assumed that dry stem biomass is 47.3% carbon (Martin and Thomas 2011). Where height data were not available, it was estimated by applying the Feldpausch et al. (2011) allometric equation.
	Branch turnover net primary productivity ($NPP_{\mathrm{branch\ turnover}}$)	See RAINFOR-GEM manual (2012, p. 61) for description of decomposition status and surface area formulas.
	Litterfall net primary productivity ($NPP_{\mathrm{litterfall}}$)	$NPP_{\mathrm{litterfall}}$ was determined as: $NPP_{\mathrm{litterfall}} = NPP_{\mathrm{canopy}} -$ Loss to leaf herbivory. Litterfall was separated into its components, oven dried at 80 °C to constant mass and weighed. Litter was estimated to be 49.2% carbon, based on mean Amazonian values (S. Patiño, unpublished analysis).
	Leaf area index (LAI)	LAI estimated using true LAI output from the CAN-EYE software which account for clumping of foliage, and assuming a fixed leaf inclination angle of 42.5°, based on mean estimates from ESP. Leaves were separated into sunlit and shaded fractions using the following equation: $F_{\mathrm{sunlit}} = (1\text{-}\exp(\text{-}K^{*}\mathrm{LAI}))/K$ where K is the light extinction coefficient, and F_{sunlit} is the sunlit leaf fraction (Doughty and Goulden 2008). The model assumptions are randomly distributed leaves, and $K = 0.5/\cos(Z)$, where Z is the solar zenith angle, which was set to 30° in this study.
	Loss to leaf herbivory ($NPP_{\mathrm{herbivory}}$)	The fractional herbivory (H) for each leaf was calculated as: $H = (A_{\mathrm{nh}} - A_{\mathrm{h}})/A_{\mathrm{nh}}$, where A_{h} is the area of each individual leaf including the damage incurred by herbivory and A_{nh} is the leaf area prior to herbivory. The mean values of H were calculated across all leaves collected both per litterfall trap and per plot.
Below-ground net primary productivity (NPP_{BG})	Coarse root net primary productivity ($NPP_{\mathrm{coarse\ roots}}$)	See RAINFOR-GEM manual (Version 2.2, 2012, p.47) for description and range of root:shoot ratio.
	Fine root net primary productivity ($NPP_{\mathrm{fine\ roots}}$)	Roots were manually removed from the soil samples in four 10 min time steps, according to a method that corrects for underestimation of biomass of hard-to-extract roots (Metcalfe et al. 2007) and used to predict root extraction beyond 40 min (up to 100 min); we estimate that there was an additional 34% correction factor for fine roots not collected within 40 minutes. No correction was applied for fine root productivity below 30 cm.
Autotrophic (R_{a}) and hetertrophic (R_{h}) respiration	Total soil CO_2 efflux (R_{soil})	Soil surface temperature (T260 probe, Testo Ltd., Hampshire, UK) and moisture (Hydrosense probe, Campbell Scientific Ltd., Loughborough, UK) were recorded at each point after efflux measurement.
	Soil CO_2 efflux partitioned into autotrophic ($R_{\mathrm{rhizosphere}}$) and heterotrophic (R_{soilhet}) components	The partitioning experiment allows estimation of the relative contributions of (1) surface organic litter, (2) roots, (3) mycorrhizae and (4) soil organic matter to total soil CO_2 efflux. Contributions are estimated from differences between collars subjected to different treatments, in excess of pre-existing spatial variation.
	Canopy respiration (R_{leaves})	To scale to whole-canopy respiration, mean dark respiration for shade and sunlit leaves were multiplied by the respective estimated fractions of total LAI. The wet season respiration mean was applied to all months with >100 mm rain; the dry season months, measured dry season respiration was linearly scaled by the soil moisture saturation to allow for more continuous variation of leaf respiration. To account for daytime light inhibition of leaf dark respiration, we applied an inhibition factor: 67% of daytime leaf dark respiration, 34% of total leaf dark respiration (Malhi et al. 2009). These were calculated by applying the Atkin et al. (2000) equations for light inhibition of leaf respiration to a plot in Tapajós forest in Brazil (Malhi et al. 2009; Lloyd et al. 2010).
	Above-ground live wood respiration (R_{stems})	To estimate plot-level stem respiration tree respiration per unit bole area was multiplied by bole surface area index (SAI) for each tree, estimated with the following equation (Chambers et al. 2004): $\log_{10}(\mathrm{SA}) = -0.105 - 0.686\log(\mathrm{DBH}) + 2.208\log(\mathrm{DBH})^2 - 0.627\log(\mathrm{DBH})^3$, where H is tree height, and DBH is bole diameter at 1.3 m height. Finally, for all 25 trees together we regressed mean annual bole respiration against total annual growth.
	Coarse root respiration ($R_{\mathrm{coarse\ roots}}$)	Estimated by multiplying measured above-ground live wood respiration by 0.21.

Table 4. Annual averaged canopy *NPP*, branch *NPP*, stem *NPP*, coarse root *NPP*, fine root *NPP*, total above-ground *NPP*, total below-ground *NPP*, total *NPP*, canopy dark respiration, wood respiration, root respiration, coarse woody respiration, total autotrophic respiration, total heterotrophic respiration, total respiration, fraction of respiration above-ground and fraction below ground, *NPP*, *GPP* and *CUE* for 2 years of data for San Pedro tropical montane forest plots at 1500 m and 1750 m, Peru, 2009–2010. All values are in Mg C ha^{-1} $year^{-1}$, unless otherwise stated. We report two primary types of uncertainty. Error is the sampling uncertainty associated with the spatial heterogeneity of the study plot and the limited number of samples. Total error also includes the systematic uncertainty associated with either unknown biases in measurement, or uncertainties in scaling measurements to the plot level.

	SP1500 Mean	Sample error	Total error	SP1750 Mean	Sample error	Total error
$NPP_{\text{litterfall}}$	5.33	0.22	0.22	3.52	0.24	0.24
NPP_{leaves}	4.12	0.18	0.18	2.63	0.17	0.17
NPP_{flowers}	0.16	0.03	0.03	0.03	0.00	0.00
NPP_{fruit}	0.19	0.04	0.04	0.15	0.02	0.02
NPP_{twigs}	0.70	0.05	0.05	0.52	0.10	0.10
$NPP_{\text{herbivory}}$	0.66	0.03	0.03	0.42	0.03	0.03
$NPP_{\text{bromeliads}}$	0.00	0.00	0.00	0.01	0.00	0.00
$NPP_{\text{other epiphytes}}$	0.06	0.01	0.01	0.12	0.03	0.03
$NPP_{\text{branch turnover}}$	0.52	0.07	0.07	0.38	0.04	0.04
$NPP_{\text{acw > 10cm dbh}}$	2.89	0.29	0.29	1.72	0.17	0.17
$NPP_{\text{acw < 10cm dbh}}$	0.04	0.00	0.00	0.15	0.02	0.02
$NPP_{\text{coarse roots}}$	0.61	0.06	0.06	0.36	0.04	0.04
$NPP_{\text{fine roots}}$	1.89	0.30	0.30	1.22	0.23	0.23
R_{leaf}	7.06	1.29	2.48	6.55	0.93	2.17
R_{stem}	8.91	0.90	2.82	9.70	0.97	3.07
$R_{\text{rhizosphere}}$	8.79	1.04	1.36	6.11	0.74	0.96
$R_{\text{coarse roots}}$	1.87	NA	0.95	2.04	NA	1.02
$R_{\text{soil het}}$	4.63	0.52	0.70	4.37	0.44	0.62
R_{soil}	13.42	1.16	1.16	10.47	0.86	0.86
R_{a}	26.63	1.90	4.10	24.40	1.55	4.01
NPP	11.94	0.47	0.47	7.92	0.38	0.38
GPP	38.57	1.96	4.13	32.33	1.60	4.03
CUE	0.31	0.02	0.04	0.25	0.02	0.03

*$NPP_{\text{litterfall}}$ includes unidentified components, accounting for the discrepancy between total $NPP_{\text{litterfall}}$ and the sum of NPP canopy components.

Amazonia (Figure 1) – this value is higher than those previously reported for this site (e.g. in Girardin et al. 2010), a result of the more complete and gap-filled dataset. The high rainfall at the base of the Andes in this region occurs because of the convergence of warm, moist air from lowland Amazonia with cold katabatic flows down the slopes of the Andes, forming a frontal rain system and resulting in peaks of rainfall in the early morning (Killeen et al. 2007; Rapp and Silman 2012). In the peak of the wet season (austral summer, December–March), rainfall rates were >600 mm $month^{-1}$, and even in the dry season (austral winter) rainfall rates were 200–300 mm $month^{-1}$, much higher than that found in the rainy season in many lowland rainforests. Hence San Pedro appears to have no water-limited 'dry season'. Instead, the temperature seasonality allows us to refer to seasons as a short austral winter (May–August) and long austral summer (September–April), with corresponding seasonality in solar radiation (high in summer, low in winter). Solar radiation seasonality is mainly explained by the seasonality of cloud cover, the forest is immersed in the cloud base during the winter months resulting in a strong solar radiation minimum in June (Figure 1). The average annual air temperature was 18.8 ± 0.02 °C (1500 m) and 17.43 ± 0.02 °C (1750 m), usually with <5 °C diurnal and seasonal variation around this mean. Lowest temperatures were found in the austral winter (May–July), a result of occasional incursions of cold air from the south and also frequent cloud immersion. Soil moisture showed very little seasonal variation and was high throughout the year, a consequence of high rainfall and low evapotranspiration rates. The maximum climatological water deficit was zero, with no evidence of seasonal water stress.

Carbon stocks and net primary productivity components

Above-ground coarse woody biomass and NPP_{ACW}. We estimated total above-ground biomass at 66.89/93.54 Mg C ha^{-1} for large trees (>10 cm dbh) and 5.17/5.28 Mg C ha^{-1} for small trees (<10 cm dbh). Hence, total stand level above-ground biomass was 72.05/98.82 Mg C ha^{-1}.

The average NPP_{ACW} from large trees (>10 cm) was greater at 1500 m than at 1750 m (2.89 ± 0.29/1.72 ± 0.17 Mg C ha^{-1} $year^{-1}$, Table 4). That from small trees was smaller at 1500 m than at 1750 m (0.04 ± 0.003/0.15 ± 0.02 Mg C ha^{-1} $year^{-1}$). Hence, total estimated NPP_{ACW} was 2.93 ± 0.29 at 1500 m and 1.87 ± 0.17 at 1750 m.

Both plots displayed a clear seasonal pattern of NPP_{ACW} with a broad minimum in stem productivity observed during the coolest and low-cloud base period (June–August) and highest productivity recorded over summer (Figure 2). To estimate the effect of moisture expansion during the wet season on tree growth, we separated the trees with almost no annual growth (NPP_{ACW} < 0.05 kg C $tree^{-1}$

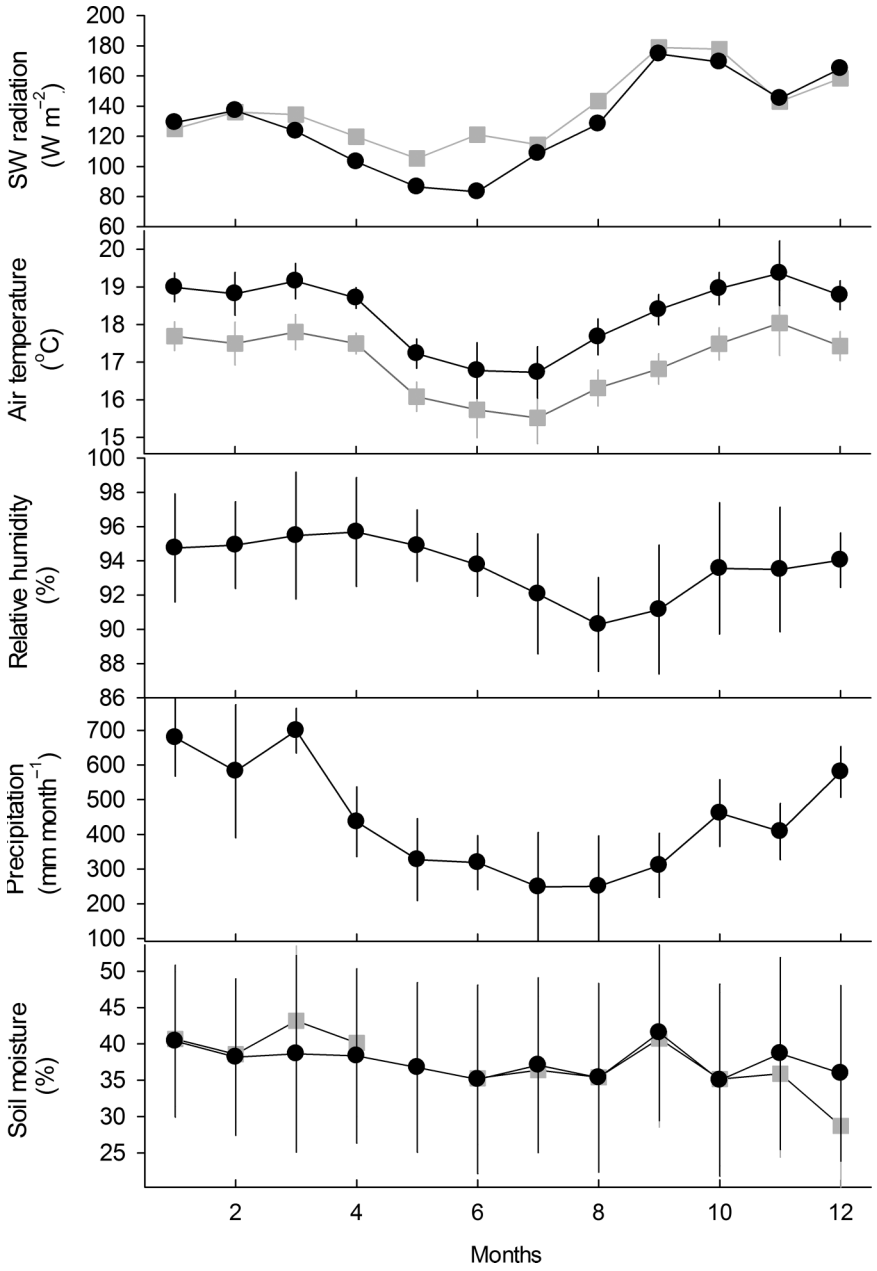

Figure 1. Climate data from a meteorological station located in a clearing ca. 1 km from SP 1500, temperature (T260 probe, Testo Ltd., Hampshire), and soil moisture (Hydrosense probe, Campbell Scientific Ltd.) from SP 1500 (black circles) and SP 1750 (grey circles). San Pedro, Peruvian Andes, from 2009–2011. (a) total radiation (W m^{-2}), (b) average monthly temperature (°C), (c) atmospheric relative humidity (%), (d) average monthly precipitation (mm) and (e) soil moisture (%). Error bars show ±1 SD.

year^{-1}, $N = 106$ at 1500 m, $N = 81$ at 1750 m) and measured their seasonal trends. We estimated that the seasonal effect of moisture expansion during the winter (April–November) was marginally lower at 1500 m (0.002 Mg C ha^{-1} year^{-1}) than at 1750 m (0.019 Mg C ha^{-1} year^{-1}). Even after correcting for moisture expansion, there was a moderately strong seasonality in both plots, ranging from 0.18 ± 0.01 to 0.28 ± 0.02 Mg C ha^{-1} month^{-1} at SP 1500, and from 0.12 ± 0.01 to 0.17 ± 0.01 Mg C ha^{-1} month^{-1} at SP 1750. We estimated stem biomass residence times of 24/53 years by dividing above-ground live coarse woody (ACW) biomass by NPP_{ACW}. These estimates are at the lower range of values (27.54–102.05 years) reported from old-growth forests in South American lowland Amazonia (Malhi et al. 2004; Keeling and Phillips 2007; da Costa et al. 2010; Galbraith et al. 2013).

Canopy net primary productivity (NPP_{canopy}*).* NPP_{canopy} was greater at 1500 m than at 1750 m ($P < 0.001$, $5.99 \pm 0.22/3.94 \pm 0.24$ Mg C ha^{-1} year^{-1}), with low within-plot variability. This difference was principally driven by NPP_{leaves}. Twigs, bromeliads and reproductive components (flower and fruit) showed no difference between plots. NPP_{canopy} was mainly allocated to leaves (77%/75%).

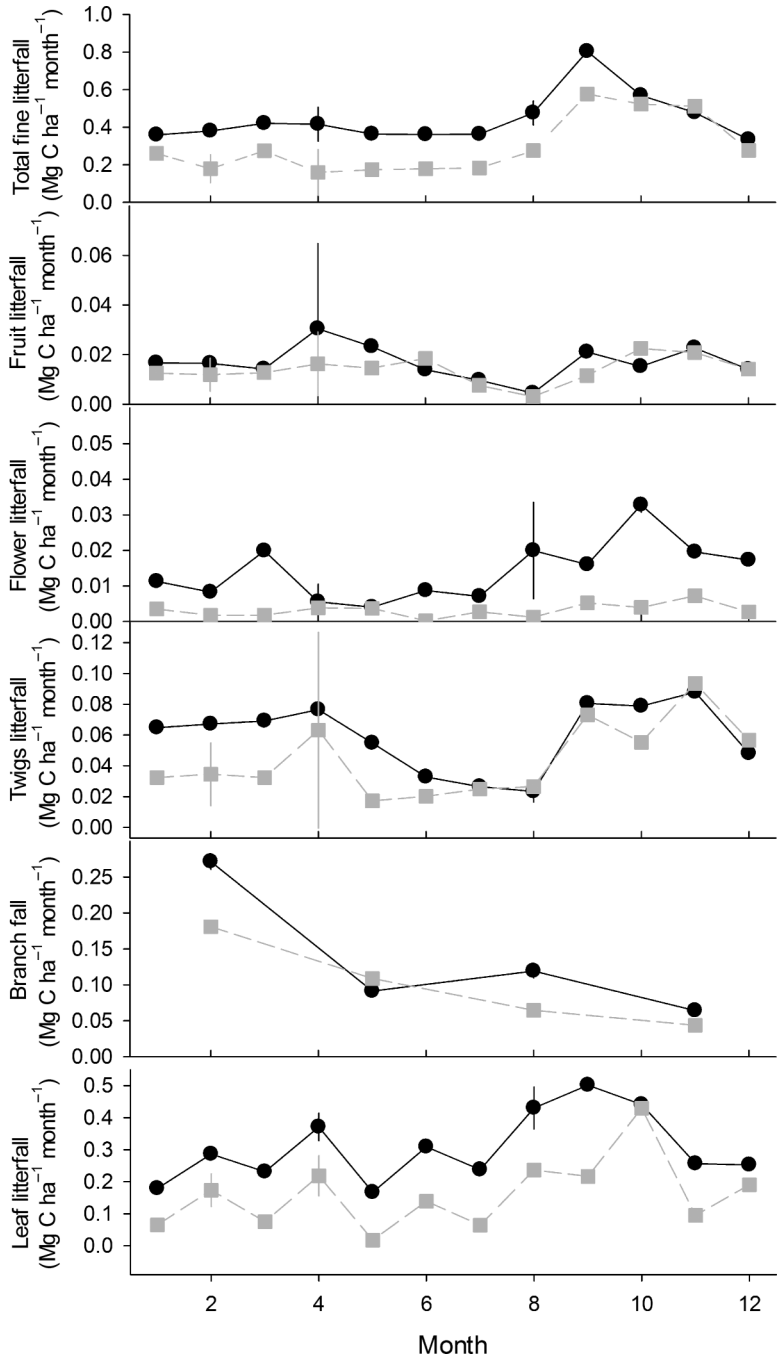

Figure 2. Sum of the monthly collections from 25 litter traps of total fine litterfall, fruit, flower, twigs, branch, leaves *NPP* (Mg C ha^{-1} month^{-1}) for SP 1500 (black circles, 2007–2011) and SP 1750 (grey squares, 2009–2011), San Pedro, Peruvian Andes. Error bars show ±1 SE.

The remaining canopy productivity was allocated to twigs (13%/15%), reproductive organs (7%/5%), and lost to herbivory (12%/12%).

Total litterfall showed evidence of seasonality at both sites, with a peak in litterfall coinciding with the transition season (August–October), at the peak of solar radiation (Figures 1 and 3). Peak litterfall rates were 0.6/0.8 Mg C ha^{-1} month^{-1} (September) and dropped to 0.21/0.39 Mg C ha^{-1} month^{-1} at the end of the austral summer. Leaf, twig, and reproductive organ litterfall showed evidence of a weak seasonal peak towards the end of the austral winter (August–December) and at the start of winter (March–April). Leaf and flower litterfall showed a similar peak in August–October, although flower fall also showed a smaller secondary peak at one site in March. Fruit litterfall showed two smaller peaks, one in the March–May transition and in the August–October transition (periods of highest sunshine). Twig fall was at a minimum in the austral winter, and showed a strong peak from January–March. Austral winter is the period of lowest cloud base

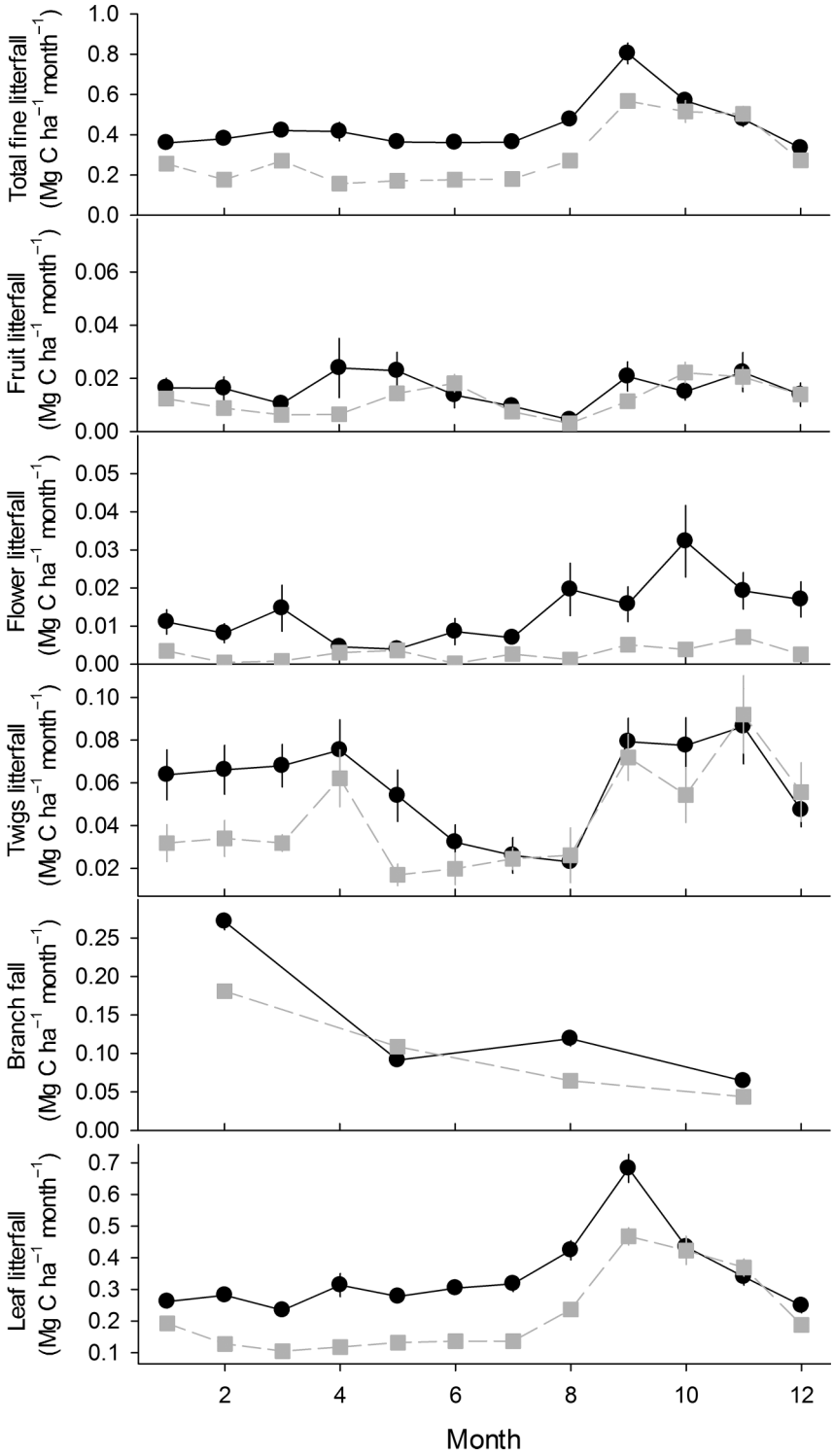

Figure 3. Above-ground woody net primary productivity (NPP_{ACW}, Mg C ha^{-1} month^{-1}) using dendrometer bands measured every 3 months over a 2-year period for SP 1500 (black circles, 2007–2011) and SP 1750 (grey squares, 2009–2011), San Pedro, Peruvian Andes. Error bars are ±1 SE, assuming that each measurement on each tree is accurate to 1 mm.

heights and most frequent cloud immersion, whereas cloud base heights are frequently above the mountains in the austral summer. Hence the broad maximum of all litterfall components at both San Pedro plots coincides with the end of the low-cloud immersion period and the peak in solar radiation levels. Seasonal amplitude (max – min) of NPP_{canopy} is more pronounced at SP 1750, consistent with the hypothesis that this upper site experiences greater cloud immersion.

Herbivory. We recorded a mean herbivory fraction of 16.0 ± 0.2/15.9 ± 0.1%. Correcting the measured NPP_{leaves} in both plots according to this fraction, we estimated an *NPP* loss to leaf herbivory of 0.66 ±

0.03/0.42 ± 0.03 Mg C ha^{-1} year^{-1}. This relatively large term emerges from a combination of the high herbivory fraction and the high rates of leaf production. As we do not provide estimates of leaf herbivory on a seasonal timescale, we do not include herbivory loss in our estimates of monthly NPP_{canopy}.

Leaf area index and leaf production. The leaf area index (LAI) in SP 1500 (not shown) showed a weak seasonal trend, averaging 4.72 ± 0.20 m^2 m^{-2} in the austral winter (June–October), and 5.25 ± 0.20 m^2 m^{-2} in the austral summer. In SP 1750, LAI was not seasonal, ranging from 5.02 ± 0.21 in the austral winter to 5.20 ± 0.19 m^2 m^{-2} in the austral summer. Annual LAI averaged 4.93 ± 0.20/5.09 ± 0.20 m^2 m^{-2}. In both plots, leaf shedding (litterfall) began in August/September, matched by a decline in LAI. Leaf shedding peaked in September and LAI reached a minimum shortly after, in October. Thereafter, leaf shedding decreased as LAI increased, indicating the production of new leaves.

Fine root net primary production ($\text{NPP}_{\textit{fine roots}}$*).* Fine root growth showed a strongly seasonal cycle, different to that of stem and canopy productivity, with highest growth in the austral summer in both plots, decreasing by 52%/41% from February–July (Figure 4). Total fine root productivity was higher at the lower elevation plot, averaging 1.89 ± 0.30/1.22 ± 0.23 Mg C ha^{-1} year^{-1} at SP 1500/SP 1750 (Table 4).

Annual coarse root productivity ($\text{NPP}_{\textit{coarse roots}}$*).* Annual coarse root productivity was estimated as a fraction of above-ground productivity. Hence, we report significantly higher coarse root production at SP 1500 than SP 1750 (0.61 ± 0.06/0.36 ± 0.04 Mg C ha^{-1} year^{-1}). Measurements over 2 years indicated a strong seasonal pattern in both plots, with root growth significantly greater in January than in July ($P < 0.001$, Figure 4).

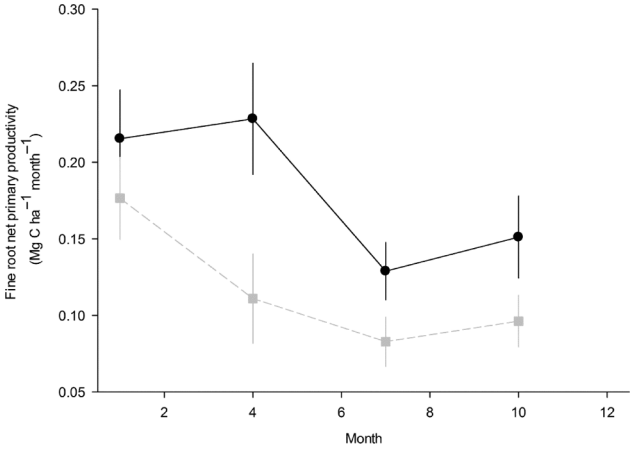

Figure 4. Fine root net primary productivity ($NPP_{\text{fine roots}}$, Mg C ha^{-1} month^{-1}) from 16 ingrowth cores collected every three months over a 2-year period for SP 1500 (black circles, 2007–2011) and SP 1750 (grey squares, 2009–2011), San Pedro, Peruvian Andes. Error bars show ±1 SE.

In both plots, $NPP_{\text{fine roots}}$ peaked at the height of summer (January/April) and declined over the austral winter, following the seasonality trend of NPP_{ACW}.

Seasonality of NPP. Figure 5 shows the seasonal budget of *NPP* and its components. At SP 1500, the overall growth rate remained relatively constant throughout the year, ranging from 1.03 ± 0.10 to 1.39 ± 0.11 Mg C ha^{-1} month^{-1}. NPP_{total} decreased slightly at the end of the austral winter. At SP 1750, there was a strong seasonal signal of the overall growth rate: total *NPP* is driven by $NPP_{\text{litterfall}}$ seasonality and matches solar radiation seasonality. Overall growth rates decreased during the austral winter, peaking at the start of summer, when solar radiation is high.

Autotrophic and heterotrophic respiration

Total soil CO_2 efflux. Below-ground, total mean annual autotrophic respiration was significantly higher at SP 1500, mainly driven by a difference in $R_{\text{rhizosphere}}$ (Table 4). Total soil respiration had a significant ($P < 0.001$) seasonal cycle and was lowest during the austral winter at both sites averaging 1.07/0.83 Mg C ha^{-1} month^{-1} (May–September) and increased to 1.30/1.02 Mg C ha^{-1} month^{-1} during the austral summer (Figure 6).

Autotrophic and heterotrophic components of soil respiration (R_a *and* R_h*).* We calculated the average respiration fraction attributable to the rhizosphere by using the results of the respiration partitioning experiment (Table 2). Monthly values of tubes excluding rhizosphere respiration (40 cm depth) were subtracted from monthly values of tubes including rhizosphere and heterotrophic respiration (10 cm depth). Mean monthly absolute values of root respiration accounted for 65%/58% of soil respiration. This fraction varied seasonally, averaging 62%/54% from June–October and 67%/61% for the rest of the year. Total rhizosphere respiration had a significant seasonal cycle ($P < 0.001$) and was lowest between May and September at both sites, averaging 0.69/0.49 Mg C ha^{-1} month^{-1} and 0.86/0.59 Mg C ha^{-1} month^{-1} during the rest of the year. Total mean annual rhizosphere respiration was higher ($P < 0.001$) at SP 1500 than SP 1750 (Table 4). Total heterotrophic soil respiration had a significant seasonal cycle ($P < 0.001$) and was lowest between March and September at both sites averaging 0.38/0.34 Mg C ha^{-1} month^{-1} and 0.43/0.44 Mg C ha^{-1} month^{-1} during the rest of the year (Figure 6). Total mean annual soil respiration was higher ($P < 0.001$) at SP 1500 than SP 1750 (Table 4).

To control for the effect of the mixing of the soil on our partitioning experiment, we investigated the effect of a disturbance on soil cores. Total soil respiration for the undisturbed SP 1500 cores were significantly lower ($P < 0.01$), increasing by 18% from an average of 2.22 ± 0.11 μmol m^{-2} s^{-1} to 2.69 ± 0.12 μmol m^{-2} s^{-1} for the disturbed cores. At SP 1750, there was no significant difference ($P > 0.05$) between the undisturbed cores (3.45 ± 0.15 μmol m^{-2} s^{-1}) and the disturbed cores (3.58 ± 0.15 μmol

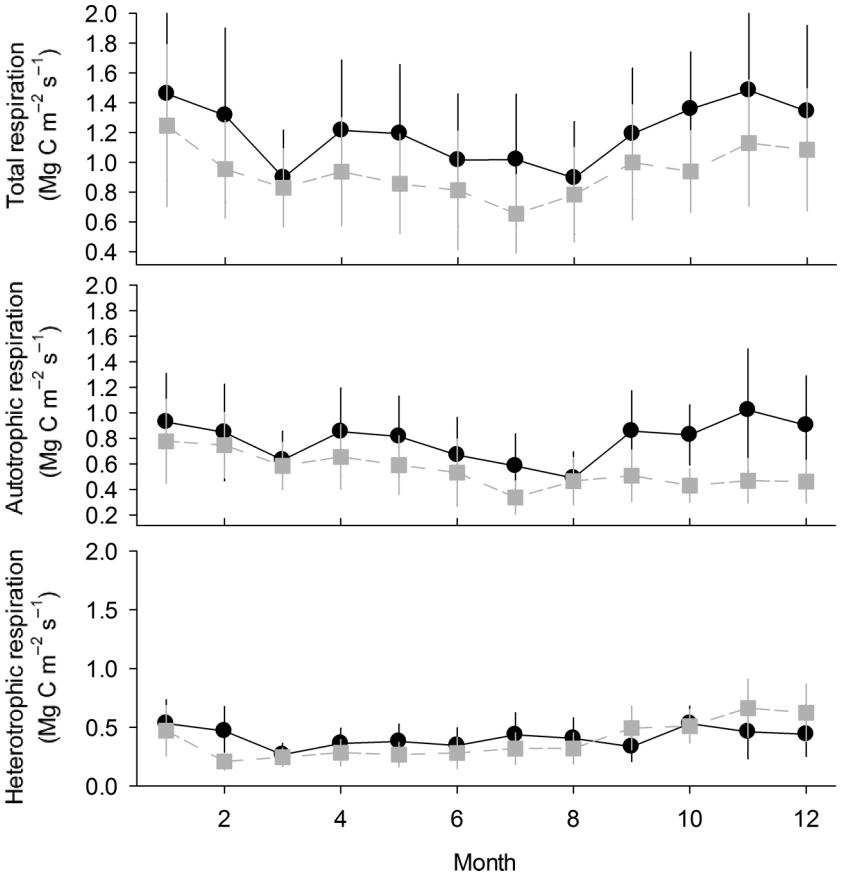

Figure 5. (top) Total soil respiration from 25 collars measured monthly, (middle) autotrophic respiration and (bottom) heterotrophic respiration (Mg C m^{-2} s^{-1}) from a 2-year period from SP 1500 (black circles, 2007–2011) and SP 1750 (grey squares, 2009–2011), San Pedro, Peruvian Andes. Autotrophic respiration is determined by an exclusion experiment ($N = 16$) where respiration was measured from tubes from which roots and mycorrhizae were removed. Error bars show ±1 SE.

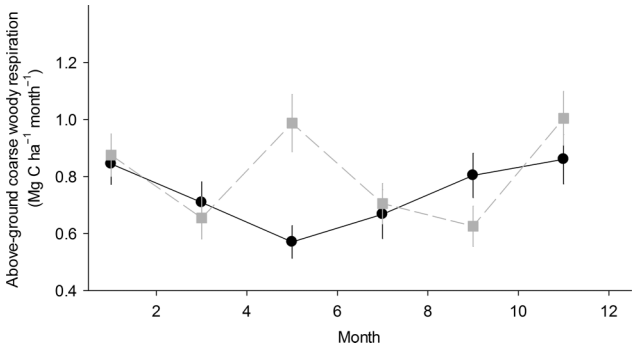

Figure 6. Above-ground wood respiration in Mg C ha^{-1} month^{-1} in SP 1500 (black circles, 2007–2011) and SP 1750 (grey squares, 2009–2011) from collars on 25 trees measured every 2 months and multiplied by the total woody surface area of the plot, San Pedro, Peruvian Andes. We scaled total respiration by NPP_{ACW} to account for varied tree growth rates. Error bars show ±1 SE multiplied by woody surface area.

m^{-2} s^{-1}), a difference of 4%. There was no significant trend ($P > 0.05$) in this difference with time in both plot, and no significant seasonal trend (see online supplemental material).

Canopy respiration. Although we observed a mild seasonal cycle, sunlit leaf dark respiration measurements showed a significant difference between plots during June, but not October (Table 5). Similarly, shaded leaf dark respiration measurements showed no significant difference between plots in either season. Sunlit leaves showed significant seasonality, with higher respiration in winter. We did not find a significant relationship ($P > 0.05$) between stem *NPP* and dark leaf respiration. Light-saturated sunlit leaf photosynthesis showed significant seasonality.

There was no strong seasonality in canopy respiration. Mean monthly canopy respiration was estimated at 0.82/0.76 Mg C ha^{-1} month^{-1} between May and September and at 0.92/0.85 during the rest of the year (not shown). We multiplied our results by a factor of 0.67 to correct for light inhibition of daytime respiration. Total mean annual canopy respiration was higher at SP 1500 than SP 1750 (Table 5).

Above-ground live coarse woody respiration (R_{stem}). Total ACW surface area of large trees (>10 cm DBH) was estimated at 17,427/21,349 m^2 ha^{-1}, with a height adjustment to the Chambers equation of 0.72/0.80 (Robertson et al. 2010). Total ACW surface area of small trees (<10 cm

Table 5. Leaf dark respiration values (μmol m^{-2} s^{-1}), by season and by leaf position (sun vs. shade) in two tropical montane forest plots at San Pedro (SP 1500 and SP 1750), Cusco, Peru, 2010. Dry season is from May to September, wet season is from October to April. These respiration values are the values the leaf would respire theoretically at the mean annual temperature of the site (12.5 °C). Significance between plots is denoted by: *, $P < 0.05$; **, $P < 0.01$; ***, $P < 0.001$.

	Winter sun	Winter shade	Summer sun	Summer shade	Winter max shotosynthesis	Summer max shotosynthesis
SP1750	0.69* ± 0.07	0.37 ± 0.04	0.61 ± 0.07	0.47 ± 0.07	7.95* ± 0.47	5.78 ± 0.82
SP1500	0.43* ± 0.05	0.32 ± 0.05	0.71 ± 0.09	0.48 ± 0.10	6.38* ± 0.36	5.15 ± 0.46

DBH) was 1378/1506 m^2 ha^{-1}. This summed to a total ACW area of 18,805/22,728 m^2 ha^{-1}. Based on this result, we estimated an ACW area index (SAI) of 1.80/1.99.

To scale R_{stem} measurements to the plot level, we established a relationship between NPP_{ACW} and R_{stem} for the 25 trees sampled. We found that the trees measured for R_{stem} grew faster than average; hence we reduced our estimates for respiratory fluxes by 12% at both plots when scaling to 1 ha. We then multiplied total plot ACW surface area by our scaled ACW respiration fluxes (Figure 7).There was a significant seasonal cycle in wood respiration at both sites ($P < 0.001$). However, the seasonal cycle was not obviously related to precipitation seasonality, with respiration peaking in summer at SP 1500 and at the start of austral winter and in the austral summer at SP 1750 (Figure 7). There was no significant difference between the sites when compared on a monthly timescale ($P > 0.05$). Annual R_{stem} was significantly greater ($P < 0.05$) at 1500 m than at 1750 m, averaging 8.91 ± 2.82/9.70 ± 3.07 Mg C ha^{-1} $year^{-1}$ for all our measurements.

Overall carbon budget

We found a number of significant differences in the carbon cycle between the two plots (Table 4, Figure 8). Canopy, stem and fine root *NPP* were significantly higher at SP 1500 than at SP 1750. As a result, total *NPP* was 1.5 times higher at SP 1500 than SP 1750, averaging 11.94 ± 0.47/7.92 ± 0.38 Mg C ha^{-1} $year^{-1}$. In terms of CO_2 efflux, leaf, stem and rhizosphere respiration were higher at SP 1500. As a result, R_a was significantly higher at SP 1500 than at SP 1750 (26.63 ± 4.10/24.40 ± 4.01 Mg C ha^{-1} $year^{-1}$). The high *NPP* and R_a values drove our estimate of *GPP* up at SP 1500 (38.57 ± 4.13/32.33 ± 4.03 Mg C ha^{-1} yr^{-1}, a difference of 6.24 Mg C ha^{-1} $year^{-1}$). *CUE* was 1.2 higher at SP 1500 than SP 1750, averaging 0.31 ± 0.04/0.25 ± 0.03 Mg C ha^{-1} $year^{-1}$.

Discussion

Intensive plots monitoring: seeking a comprehensive approach to quantifying the carbon budget

The two San Pedro plots we focused on in this study are part of a network of intensive carbon-monitoring plots in which we have measured all the main components of *NPP* and respiration (autotrophic and heterotrophic) to improve our mechanistic understanding of the internal components of the carbon cycle and how they interact with environmental variables. This paper presents the first complete measurements of the main components of *NPP*, respiration and their variation over a seasonal cycle in two tropical montane forest plots located at the base of the cloud immersion zone. A detailed time series of these components collected over 3–5 years (Table 2) allowed us to present the first in-depth study of seasonal variation of the carbon budget at the base of a montane forest cloud immersion zone. Our approach of intensive carbon cycling monitoring provides a complete overview of the carbon cycle: we provide a 'bottom-up' estimate of *GPP* by summing the rate of carbon assimilated into biomass (*NPP*) and emitted through autotrophic respiration (R_a). Although these two plots are located within 1 km of each other, they differ in terms of biomass, *NPP* and *GPP*. Despite the difference in total *NPP* between the two plots, we found no variation in allocation of *NPP* to canopy (50%/50%), above- and below-ground coarse wood (34%/35%) and fine roots (15%/15%) between the two plots (Table 6). Thus, for a given *NPP* component, the same fraction of *NPP* was allocated in both plots, although growth was substantially slower at SP 1750. These results can be compared with the conclusions of a review of *NPP* allocation from 35 tropical forest sites, in which Malhi et al. (2011) reported that *NPP* allocation to the canopy remained relatively invariant in all sites (ca. 25–45%). Nonetheless, the canopy allocation reported here is larger than the pantropical mean reported by Malhi et al. (2011); this is partially explained by the inclusion of herbivory to our NPP_{canopy}, as *NPP* allocated to the canopy without herbivory was 45%/44%, towards the upper end of the range reported by Malhi et al. (2011).

The NPP_{total} reported here is significantly higher than our previous estimates from SP 1500 (7.06 ± 0.44 Mg C ha^{-1} $year^{-1}$ (Girardin et al. 2010), a difference driven by NPP_{canopy} (which now includes herbivory), $NPP_{ACW<10cm}$ (now directly measured), $NPP_{branch\ turnover}$ (now directly measured) and $NPP_{fine\ roots}$ (now corrected for root depth). The R_h and R_a values reported here also take precedence over our previous estimates, as they are directly measured from a partitioning experiment. A more complete intensive measurement regime, combined with inter-annual variability may explain an increase in *NPP* (and hence *GPP*) estimates between studies, hence the values reported here take precedence over our previously reported estimates (Girardin et al. 2010; Malhi 2012). We are fairly confident

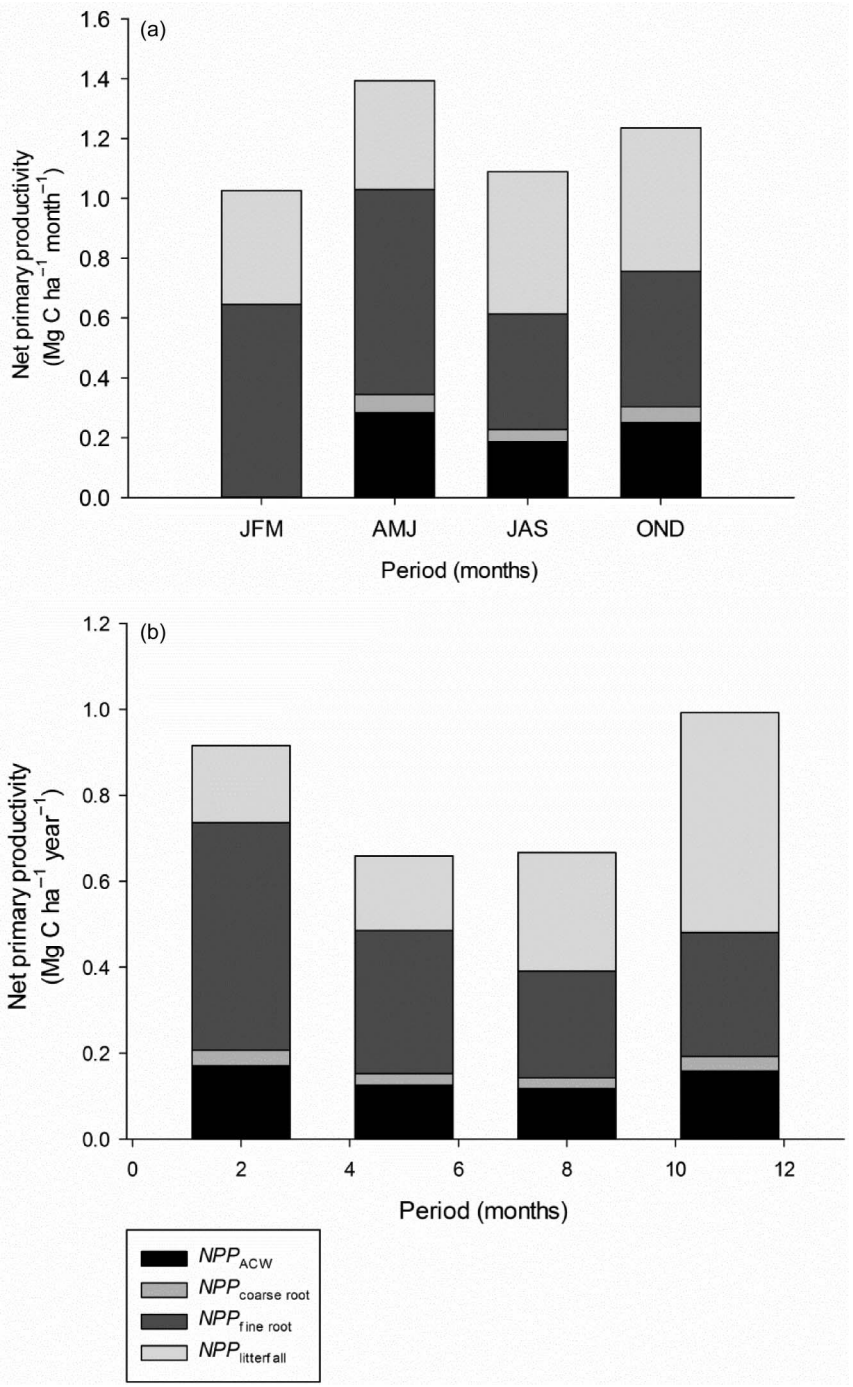

Figure 7. Seasonality of above-ground coarse woody material (ACW), coarse roots, fine roots and litterfall *NPP* in SP 1500 (top, 2007–2011) and SP 1750 (bottom, 2009–2011), San Pedro, Peruvian Andes. Error bars show ±1 SE.

that *NPP* terms and R_{soil} are measured precisely and sampled without large biases. The uncertainty associated with these components is sampling uncertainty, a term which can be reliably estimated (Table 4). The largest sources of uncertainty in our measurement approach are associated with leaf respiration (both daytime inhibition and scaling) and stem respiration (scaling from point measurements to the whole stem surface), both of which feed through to higher uncertainty in autotrophic respiration. The issues surrounding scaling of leaf and stem respiration certainly warrant further research.

Seasonal trends and climatic drivers of NPP *and* R_a *components*

We quantified the seasonal budget of each *NPP* component in both plots (Figure 5). Here, we assumed that the peak in canopy production was synchronised with the peak in litterfall ($NPP_{litterfall}$), a feature which has been demonstrated in several sites in lowland Amazonia (Doughty and Goulden 2008; Malhi et al. 2014) but which we cannot yet confirm at this site. SP 1500 showed high seasonality in ACW, fine roots and fine litter *NPP* as reported for most forests located below the cloud base.

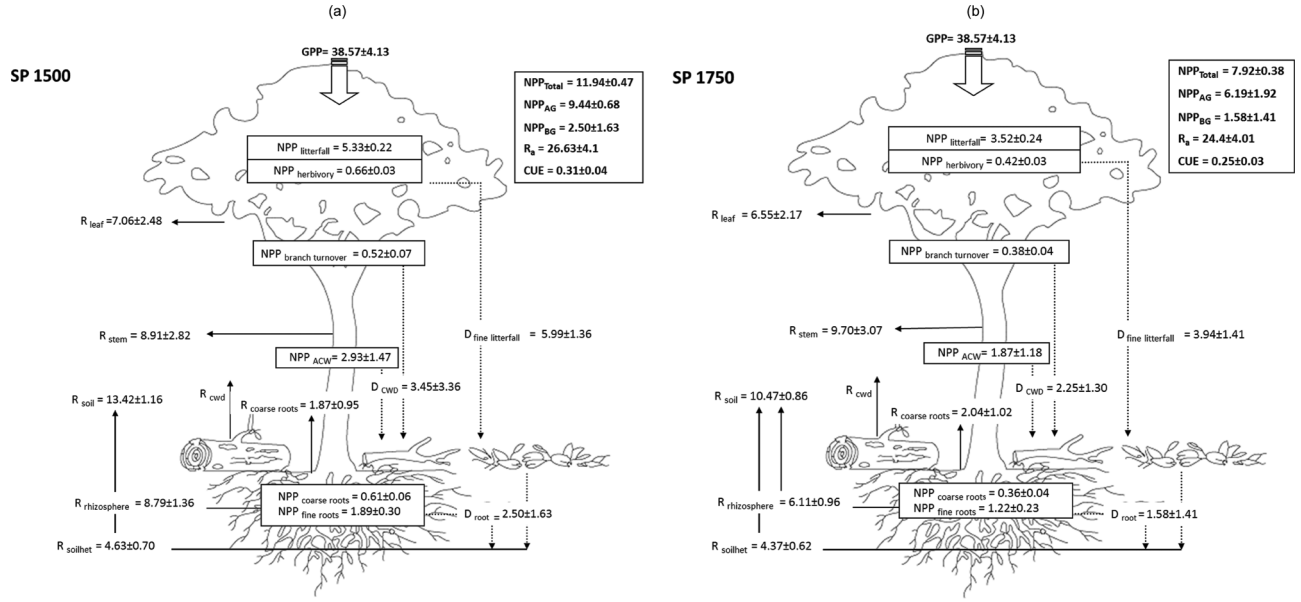

Figure 8. Mean annual values for components of autotrophic respiration, *NPP*, GPP and *CUE* at SP 1500 (2007–2011) and SP 1750 (2009–2011) San Pedro, Peruvian Andes. Error bars show ±1 SE.

SP 1750 showed the low seasonality of stem and root *NPP* typically observed in montane cloud forests and a marked seasonality in NPP_{canopy} typical of lower elevation forests (C. Girardin 2013, pers comm.). We observed little seasonality in soil R_a and even less seasonal amplitude in R_h. Nonetheless, R_a increased gradually during the austral summer and decreased in the winter, indicating a close relationship between R_a and *NPP* rates (Figures 2, 4 and 6). The seasonal trend of R_a further suggests that trees invest more in biomass productivity in the cooler and darker season and more in maintenance during the warmer and high solar radiation incidence period. We lack information to accurately quantify the seasonal cycle of *CUE*. However, our data on the seasonal trends of *NPP* and R_a imply that *CUE* is likely to show no or low seasonality in both plots.

We presented the first detailed seasonal dataset of NPP_{canopy} and its components from a lower tropical montane cloud forest, allowing for interesting insights on the phenology of these lower cloud forests. The investment in photosynthetic material during the austral summer (high light incidence) may be explained by a direct need for light, or a reduction leaf pathogens pressure under drier and warmer conditions. The results presented here lead us to infer that canopy, stem and fine root productivity respond to variations in solar radiation over the year. These two plots provide a good example of a site where water availability is not a limiting factor: in forests where moisture is not a limiting factor, the phenology of the canopy responds to light availability, with increasing allocation to reproductive organs when light is in abundance (C. Girardin 2013, pers comm.).

Table 6. Carbon allocation to above- and below-ground components of *NPP* and partitioning of respiration components in two San Pedro plots (SP 1500 and SP 1750), Peru, 2009–2010. All values other than above- and below-ground carbon are fractions. SE is standard error of the mean.

Total carbon allocation	SP1500 mean (+/− SE)	SP1750 mean (+/− SE)
Above-ground carbon (Mg C ha^{-1} $year^{-1}$)	25.42 (1.62)	22.60 (1.38)
Below-ground carbon (Mg C ha^{-1} $year^{-1}$)	13.15 (1.10)	9.72 (0.80)
Above-ground fraction	0.66 (0.05)	0.70 (0.05)
Below-ground fraction	0.34 (0.03)	0.30 (0.03)
Allocation of *NPP*		
Canopy	0.50 (0.04)	0.50 (0.05)
Above-ground coarse wood	0.34 (0.07)	0.35 (0.07)
Fine roots	0.16 (0.03)	0.15 (0.03)
Partitioning of autotrophic respiration		
Canopy	0.27 (0.05)	0.27 (0.04)
Wood	0.40 (0.05)	0.48 (0.06)
Rhizosphere	0.33 (0.05)	0.25 (0.03)

*How does the base of the cloud cover impact annual carbon budgets (*NPP*,* R_a*,* GPP *and* CUE*)?*

A comparison of the overall carbon budget of these two San Pedro plots with lowland Amazonia shows that the absolute values of the main *NPP* components (ACW, fine litter and fine roots) at SP 1500 are comparable with values reported from fertile lowland Amazonian rainforests (Nepstad 2002; Chave et al. 2008; Malhi et al. 2008; Aragao et al. 2009; Malhi et al. 2014; Pasquel et al. 2014), although those of SP 1750 are closer to *NPP* estimates reported from montane forests (Girardin et al. 2014). We found a number of significant differences in the carbon cycle between the two plots. NPP_{ACW}, NPP_{canopy}, $NPP_{fine\ roots}$ and R_a were significantly higher at SP 1500 than at SP 1750, resulting in a 25% decrease in *GPP* over a 250 m elevation increase (1.37 °C decrease in temperature). Soil characteristics did not differ significantly between the two plots, hence differences in the carbon cycle between the two plots cannot be attributed to soil characteristics. Mean wood density was lower in the lower elevation plot ($0.55 \pm 0.01/0.61 \pm 0.008$ g cm^{-3} ha^{-1} (W. Farfán 2012, pers. comm.). SPD 1500 had wood density values more typical of the lowland sites, whereas SPD 1750 had values more typical of the cloud forest zone. This suggests that a distinct ecological transition occurs between 1500 and 1750 m. Recent publications from the Kosñipata elevation transect (including these two plots) present evidence of a step change in below-ground (Girardin et al. 2013a) and above-ground (C. Girardin 2013, pers comm.) productivity at the base of the cloud immersion zone, with significantly lower productivity rates and a sharp decline in tree biodiversity (Jankowski et al. 2012) in plots located within the cloud immersion zone. As a probable increase in cloud immersion frequency at SPD 1750 is the main difference between the two sites, we conclude that the distinct ecological difference between these plots is likely to be related to the cloud immersion zone rather than the linear change in temperature with increasing elevation.

We estimated that $69 \pm 19\%$ of *GPP* was allocated to R_a in SP 1500, compared with 75% in SP 1750. Hence, R_a was proportionally higher in SP 1750, resulting in a lower *CUE* value. The *CUE* of SP 1500 (0.31 ± 0.04) is typical of tropical old-growth forests, for which the ecological literature reports values of ca. 0.3 (Litton et al. 2007; Malhi 2012; Marthews et al. 2012). However, the *CUE* of SP 1750 is the lowest reported in tropical literature (0.25 ± 0.03). One possible interpretation of this is a higher allocation to metabolic processes as a result of a feature of the equilibrium environment, for example highly variable light environment (Marthews et al. 2012). Another intriguing possibility is that the forest at 1750 m is no longer at metabolic equilibrium with local climate. A similarly low value of *CUE* has been reported for an artificial drought experiment in a lowland Amazonian forest (Metcalfe et al. 2010), where it was interpreted as being partially due to net loss and emission of carbon from non-structural carbohydrate reserves. Observations and model predictions show that temperatures are rising in the region and will continue to rise (Malhi and Wright 2004; Urrutia and Vuille 2009). However, any corresponding directional change of the cloud base (cloud frequency, elevation shifts in cloud base formation) remains uncertain (Foster 2001; Rapp and Silman 2012). Our results highlight the need to understand the nature of the ecotone at the cloud base. Here, we hypothesise that the reported decrease in productivity may be driven by cloud immersion: this significant change over small distances may be explained by the fact that these two plots are distributed around the cloud base. SP 1750 is likely more frequently immersed by clouds than SP 1500, possibly explaining why carbon dynamics at SP 1750 are closer to those observed in cloud forests than lowland rainforests. While this plot displays the ecological composition of cloud montane forests, we speculate that the climate regime it experiences is shifting to that of a forest below the cloud base. Hence the climatic threshold position may already have shifted, but the tree community may not have yet. A change in cloud immersion regime resulting in a discrepancy between the ecological functioning of the forest and its climate regime may explain a low *CUE* indicative of forests out of metabolic equilibrium. However, this remains pure speculation based on the available evidence, and it is important to recognise the potential for unaccounted errors in the scaling of autotrophic respiration. Finally, the results presented here demonstrate the importance of understanding ecophysiological and ecological processes at the cloud base zone of the tropics, and the value of targeted long-term ecological and microclimate monitoring of this critical but poorly understood ecotone.

Acknowledgements

This work is a product of the RAINFOR and ABERG research consortia, and embedded within the GEM (Global Ecosystems Monitoring) network of research sites. It was funded by grants from the Gordon and Betty Moore Foundation to the Amazon Forest Inventory Work (RAINFOR) and the Andes Biodiversity and Ecosystems Research Group (ABERG), and a grant to YM and PM from the UK Natural Environment Research Council (Grant NE/D014174/1). YM is supported by the Jackson Foundation and the Oxford Martin School. We thank the Cock of the Rock Lodge at San Pedro, and Sr. Demetrio, for logistical support with this work, and INRENA for permits to conduct research in Peru.

Notes on contributors

Walter Huaraca Huasco is a botanist and plant biologist who focuses on carbon cycling in tropical forest ecosystems.

Cécile A.J. Girardin is an ecosystems scientist who focuses on carbon dynamics of tropical forest ecosystems.

Christopher E. Doughty is a junior research fellow. His main interest is understanding tropical forest carbon fluxes, through remote sensing, eddy covariance, leaf gas exchange and intensive carbon cycle plots.

Daniel B. Metcalfe is an assistant professor. He is interested in a wide range of topics broadly related to forest carbon cycling and climate.

Liliana Durand Baca; Javier E. Silva-Espejo; Darcy Galiano Cabrera; Angela Rozas Davila; Lidia P. Huaraca-Quispe; Ivonne Alzamora-Taype; Luzmila Eguiluz Mora; William Farfán-Rios; Karina Garcia Cabrera; Norma Salinas-Revilla; Luiz E.O. Aragão; Miles Silman; and Patrick Meir are tropical forest ecologists who all contributed by establishing the study areas, contributing data and advice on the interpretation of results.

Toby R. Marthews is a postdoctoral researcher. Dr Marthews's research is on forest and woodland ecosystem dynamics both through simulation work and fieldwork.

Katherine Halladay has worked on clouds and climate in the Andean transect.

Yadvinder Malhi, Senior Research Fellow and director of the Oxford Centre for Tropical Forests, leads the Ecosystems Programme of the Environmental Change Institute, with a focus of understanding the functioning of tropical forests and their response to global change.

References

Aragão LEOC, Malhi Y, Metcalfe DB, Silva-Espejo JE, Jimenez E, Navarrete D, Almeida S, Costa ALC, Salinas N, Phillips OL, et al. 2009. Above- and below-ground net primary productivity across ten Amazonian forests on contrasting soils. Biogeosciences 6:2759–2778.

Aragão LEOC, Malhi Y, Roman-Cuesta RM, Saatchi S, Anderson LO, Shimabukuro YE. 2007. Spatial patterns and fire response of recent Amazonian droughts. Geophysical Research Letters 34:7.

Atkin OK, Evans JR, Ball MC, Lambers H, Pons TL. 2000. Leaf respiration of snow gum in the light and dark interactions between temperature and irradiance. Plant Physiology 122: 915–923.

Baldocci DD. 2003. Assessing the Eddy covariance technique for evaluating carbon dioxide exchange rates of ecosystems: past, present and future. Global Change Biology 9: 479–492.

Benner J, Vitousek PM, Ostertag R. 2010. Nutrient cycling and nutrient limitation in tropical montane cloud forests. In: Bruijnzeel LA, Scatena FN, Hamilton LS, editors. Tropical montane cloud forests. Cambridge (UK): Cambridge University Press. p. 90–100.

Bruijnzeel LA, Proctor J. 1995. Hydrology and biogeochemistry of tropical montane cloud forests: what do we really know? In: Hamilton LS, Juvik JO, Scatena FN, editors. Tropical montane cloud forests. New York (NY): Springer-Verlag. p. 38–78.

Cairns MA, Brown S, Helmer EH, Baumgardner GA. 1997. Root biomass allocation in the world's upland forests. Oecologia 111:1–11.

Chambers JQ, Higuchi N, Schimel JP, Ferreira LV, Melack JM. 2000. Decomposition and carbon cycling of dead trees in tropical forests of the central Amazon. Oecologia 122:219–223.

Chambers JQ, Tribuzy ES, Toledo LC, Crispim BF, Higuchi N, dos Santos J, Araujo AC, Kruijt B, Nobre AD, Trumbore SE. 2004. Respiration from a tropical forest ecosystem: partitioning of sources and low carbon use efficiency. Ecological Applications 14:S72–S88.

Chave J, Andalo C, Brown S, Cairns MA, Chambers JQ, Eamus D, Folster H, Fromard F, Higuchi N, Kira T, et al. 2005. Tree allometry and improved estimation of carbon stocks and balance in tropical forests. Oecologia 145:87–99.

Chave J, Coomes D, Jansen S, Lewis SL, Swenson NG, Zanne AE. 2009. Towards a worldwide wood economics spectrum. Ecology Letters 12:351–366.

Chave J, Olivier J, Bongers F, Châtelet P, Forget PM, van der Meer P, Norden N, Riéra B, Charles-Dominique P. 2008. Aboveground biomass and productivity in a rain forest of eastern South America. Journal of Tropical Ecology 24:355–366.

da Costa ACL, Galbraith D, Almeida S, Portela BTT, da Costa M, de Athaydes Silva Junior J, Braga AP, de Gonçalves PHL, de Oliveira AAR, Fisher R, Phillips OL, et al. 2010. Effect of 7 yr of experimental drought on vegetation dynamics and biomass storage of an eastern Amazonian rainforest. New Phytologist 187:579–591.

Dijkshoorn JA, Huting JRM and Tempel P. 2005. Update of the 1:5 million Soil and Terrain Database for Latin America and the Caribbean (SOTERLAC; version 2.0). Wageningen (the Netherlands): ISRIC – World Soil Information.

Doughty CE, Goulden ML. 2008. Seasonal patterns of tropical forest leaf area index and CO_2 exchange. Journal of Geophysical Research-Biogeosciences 113:G00B06.

Feldpausch TR, Banin L, Phillips OL, Baker TR, Lewis SL, Quesada CA, Affum-Baffoe K, Arets EJMM, Berry NJ, Bird M, et al. 2011. Height-diameter allometry of tropical forest trees. Biogeosciences 8:1081–1106.

Foster P. 2001. The potential negative impacts of global climate change on tropical montane cloud forests. Earth-Science Reviews 55:73–106.

Galbraith D, Malhi Y, Affum-Baffoe K, Castanho ADA, Doughty CE, Fisher RA, Lewis SL, Peh KSH, Phillips OL, Quesada CA, et al. 2013. Residence times of woody biomass in tropical forests. Plant Ecology & Diversity 6:139–157.

Girardin CAJ, Aragão LEOC, Malhi Y, Huaraca Huasco W, Metcalfe DB, Durand L, Mamani M, Silva-Espejo JE, Whittaker RJ. 2013. Fine root dynamics along an elevation gradient in tropical Andean forests. Global Biogeochemical Cycles 27:252–264.

Girardin CAJ, Malhi Y, Aragao LEOC, Mamani M, Huasco WH, Durand L, Feeley KJ, Rapp J, Silva-Espejo JE, Silman M, et al. 2010. Net primary productivity allocation and cycling of carbon along a tropical forest elevational transect in the Peruvian Andes. Global Change Biology 16:3176–3192.

Girardin CAJ, Silva-Espejo JE, Doughty CE, Huaraca-Huasco W, Metcalfe DB, Galiano-Cabrera DF, Durand-Baca L, Aragão LEOC, Marthews TR, Huaraca-Quispe LP, et al. 2014. Productivity and carbon allocation in a tropical montane cloud forest of the Peruvian Andes. Plant Ecology and Diversity, 7(1–2):107–123.

Gurdak D, Rozas-Dávila A, Aragão LEOC, Huaraca Huasco W, Doughty C, Metcalfe DB, Farfan Rios W, García Cabrera K, Silva Espejo JE, Silman MRR, et al. 2014. Balancing above ground carbon fluxes and wood debris respiration to understand dynamics of biomass along a tropicaln Andes to Amazon elevational gradient. Plant Ecology and Diversity, 7(1–2):143–160.

Harmon ME, Whigham DF, Sexton J, Olmsted I. 1995. Decomposition and mass of woody detritus in the dry tropical forests of the Northeastern Yucatan Peninsula, Mexico. Biotropica 27:305–316.

Hughes IG, Hase TPA. 2010. Measurements and their uncertainties: a practical guide to modern error analysis. Oxford (UK): Oxford University Press.

Jackson RB, Canadell J, Ehleringer JR, Mooney HA, Sala OE, Schulze ED. 1996. A global analysis of root distributions for terrestrial biomes. Oecologia 108:389–411.

Jankowski JE, Merkord CL, Rios WF, Cabrera KG, Revilla NS, Silman MR. 2012. The relationship of tropical bird communities to tree species composition and vegetation structure along an Andean elevational gradient. Journal of Biogeography 40:950–962.

Keeling HC, Phillips OL. 2007. The global relationship between forest productivity and biomass. Global Ecology and Biogeography 16:618–631.

Killeen T, Douglas M, Consiglio T, Jørgensen P, Mejia J. 2007. Dry spots and wet spots in the Andean hotspot. Journal of Biogeography 34:1357–1373.

Litton CM, Raich JW, Ryan MG. 2007. Carbon allocation in forest ecosystems. Global Change Biology 13:2089–2109.

Lloyd J, Patiño S, Paiva RQ, Nardoto GB, Quesada CA, Santos AJB, Baker TR, Brand WA, Hilke I, Gielmann H, et al. 2010. Optimisation of photosynthetic carbon gain and within 1000 canopy gradients of associated foliar traits for Amazon forest trees. Biogeosciences 7:1833–1859.

Malhi Y. 2012. The productivity, metabolism and carbon cycle of tropical forest vegetation. Journal of Ecology 100(1):65–75.

Malhi Y, Aragão LEOC, Metcalfe DB, Paiva R, Quesada CA, Almeida S, Anderson L, Brando P, Chambers JQ, da Costa ACL, et al. 2009. Comprehensive assessment of carbon productivity, allocation and storage in three Amazonian forests. Global Change Biology 15:1255–1274.

Malhi Y, Baker TR, Phillips OL, Almeida S, Alvarez E, Arroyo L, Chave J, Czimczik CI, Di Fiore A, Higuchi N, et al. 2004. The above-ground coarse wood productivity of 104 Neotropical forest plots. Global Change Biology 10:563–591.

Malhi Y, Doughty C, Galbraith D. 2011. The allocation of ecosystem net primary productivity in tropical forests. Philosophical Transactions of the Royal Society 366:3225–3245.

Malhi Y, Farfán Amézquita F, Doughty CE, Silva-Espejo JE, Girardin CAJ, Metcalfe DB, Aragão LEOC, Huaraca-Quispe LP, Alzamora-Taype I, Eguiluz-Mora L, et al. 2014. The productivity, metabolism and carbon cycle of two lowland tropical forest plots in SW Amazonia, Peru. Plant Ecology and Diversity, 7(1–2):85–105.

Malhi Y, Roberts JT, Betts RA, Killeen TJ, Nobre CA. 2008. Climate change, deforestation and the fate of the Amazon. Science 319:169.

Malhi Y, Silman M, Salinas N, Bush M, Meir P, Saatchi S. 2010. Introduction: elevation gradients in the tropics: laboratories for ecosystem ecology and global change research. Global Change Biology 16:3171–3175.

Malhi Y, Wright J. 2004. Spatial patterns and recent trends in the climate of tropical rainforest regions. Philosophical Transactions of the Royal Society of London B 359:311–329.

Marthews TR, Malhi Y, Girardin CAJ, Silva-Espejo SE, Aragão LEOC, Metcalfe DB, Rapp JM, Mercado LM, Rosie A, Fisher RA, et al. 2012. Simulating forest productivity along a neotropical elevational transect: temperature variation and carbon use efficiency. Global Change Biology 18:2882–2898.

Martin AR, Thomas SC. 2011. A reassessment of carbon content in tropical trees. PlosOne 6.

Metcalfe DB, Meir P, Aragao LEOC, Lobo-do-Vale R, Galbraith D, Fisher RA, Chaves MM, Maroco JP, da Costa ACL, de Almeida SS, et al. 2010. Shifts in plant respiration and carbon use efficiency at a large-scale drought experiment in the eastern Amazon. New Phytologist 187:608–621.

Metcalfe DB, Meir P, Aragão LEOC, Malhi Y, da Costa ADL, Braga A, Gonçalves PHL, de Athaydes J, de Almeida SS, Williams M. 2007. Factors controlling spatio-temporal variation in carbon dioxide efflux from surface litter, roots and soil organic matter at four rainforest sites in the eastern Amazon. JGR-Biogeosciences 112(G4). doi:10.1029/2007JG000443

Nepstad DC. 2002. The effects of partial throughfall exclusion on canopy processes, aboveground production, and biogeochemistry of an Amazon forest. Journal of Geophysical Research 107:1–18.

Pasquel JA, Doughty CE, Metcalfe DB, Silva-Espejo JE, Girardin CAJ, Chung Gutierrez JA, Navarro Aguilar GE, Quesada CA, Hidalgo Pizango CG, Reyna Huaymacari JM, et al. 2014. The seasonal cycle of productivity, metabolism and carbon dynamics in a wet aseasonal forest in NW Amazonia (Iquitos, Peru). Plant Ecology and Diversity, 7(1–2):71–83.

Rapp JR, Silman MR. 2012. Diurnal, seasonal and altitudinal trends in microclimate across a 3900 m altitudinal gradient in the humid tropics. Climate Research 55:17–32.

Reich PB, Tjoelker MG, Walters MB, Vanderklein DW, Buschena C. 1998. Close association of RGR, leaf and root morphology, seed mass and shade tolerance in seedlings of nine boreal tree species grown in high and low light. Functional Ecology 12:327–338.

Robertson AL, Malhi Y, Farfán Amézquita F, Aragão LEOC, Silva EJ, Roberson M. 2010. Stem respiration in tropical forests along an elevation gradient in the Amazon and Andes. Global Change Biology 16:3193–3204.

Salinas N, Malhi Y, Meir P, Silman M, Roman Cuesta R, Huaman J, Salinas D, Huaman V, Gibaja A, Mamani M, et al. 2011. The sensitivity of tropical leaf litter decomposition to temperature: results from a large-scale leaf translocation experiment along an elevation gradient in Peruvian forests. New Phytologist, 189:967–977.

Taylor JR. 1997. An introduction to error analysis. The study of uncertainties in physical measurements. 2nd ed. Sausalito (CA): University Science Books.

Urrutia R, Vuille M. 2009. Climate change projections for the tropical Andes using a regional climate model: temperature and precipitation simulations for the end of the 21st century. Journal of Geophysical Research 114:D02108.

Zimmermann M, Meir P, Bird MI, Malhi Y, Ccahuana AJQ. 2009. Climate dependence of heterotrophic soil respiration from a soil-translocation experiment along a 3000 m tropical forest altitudinal gradient. European Journal of Soil Science 60:895–906.

Zimmermann M, Meir P, Bird MI, Malhi Y, Ccahuana AJQ. 2010. Temporal variation and climate dependence of soil respiration and its components along a 3000 m altitudinal tropical forest gradient. Global Biogeochemical Cycles 24:4012.